European Journal of Pharmaceutical Sciences 139 (2019) 105045

Contents lists available at ScienceDirect

European Journal of Pharmaceutical Sciences

journal homepage: www.elsevier.com/locate/ejps

Design, synthesis and anticancer evaluation of novel 1,3-benzodioxoles and 1,4-benzodioxines

Rasha Mohamed Hassan[a], Walaa Hamada Abd-Allah[b], Asmaa Mohamed Salman[c], Aida Abdel-Sattar El-Azzouny[a], Mohamed Nabil Aboul-Enein[a,*]

[a] Medicinal and Pharmaceutical Chemistry Department, Pharmaceutical and Drug Industries Research Division, National Research Centre (ID: 60014618), P.O. 12622, Dokki, Giza, Egypt

[b] Pharmaceutical Chemistry Department, College of Pharmaceutical Science and Drug Manufacturing, Misr University for Science and Technology, P.O. 77, 6th of October City, Giza, Egypt

[c] Medicinal and Pharmaceutical Chemistry Department, Pharmacology Group, Pharmaceutical and Drug Industries Research Division, National Research Centre (ID: 60014618), P.O. 12622, Dokki, Giza, Egypt

ARTICLE INFO

Keywords:
Synthesis
1,3-Benzodioxoles
1,4-Benzodioxines
Anticancer
Tubulin
Apoptosis

ABSTRACT

A new set of 1,3-benzodioxoles and 1,4-benzodioxines was designed and synthesized starting from gallic acid as anticancer agents. The antiproliferative effect of the target compounds was evaluated against a panel of cancer cell lines (HepG2, PC-3, MCF-7 and A549) using MTT assay. The 1,4-benzodioxine derivative **11a** manifested broad spectrum effect towards the four tested cancer cell lines (IC_{50} < 10 μM) with lower toxic effect on normal human cell line BJ1. Cell cycle progression of MCF-7 after treatment with compound **11a** was studied where it induced cells accumulation at G2/M phase as well as increasing in the percentage of cells at pre-G1. Compound **11a** is found to be a tubulin polymerization inhibitor with IC_{50} = 6.37 μM. Also, flow cytometeric analysis revealed that compound **11a** could induce both early and late stage apoptosis in MCF-7 cell line. Moreover, the ability of this compound to stimulate apoptosis in the latter cell line was further confirmed by: increment of Bax/Bcl-2 ratio, increase the expression of tumor suppressor gene p53, boosting the levels of initiator and executioner caspases as well as raise in the amount of cytochrome C. In addition molecular docking study was accomplished on the colchicine binding site of tubulin (pdb: 1SA0) to illustrate the interactions of the most potent compound **11a** to the receptor.

1. Introduction

Cancer is considered as one of the most serious health minatory disorders. It is ranked as one of the main reasons of global death (Torre et al., 2015; Trivedi et al., 2018). Using of available chemotherapeutic agents is commonly associated with severe side effects and drug resistance (Hao et al., 2016). Therefore, there is still a dire necessity for developing of new chemotherapeutic agents having fewer side effects.

Microtubules are cytoskeletal structures in eukaryotic cells composed of α, β-tubulin heterodimers. They play an essential role in many cellular processes such as cell division, maintenance of cell shape and cell signaling (Downing and Nogales, 1998; Fan et al., 2018). This renders microtubules an interesting target for anticancer agents. Microtubule-targeting agents are classified into two classes according to mechanism by which they interfere with microtubules dynamics. The first class is microtubule-stabilizing agents such as taxens which promote microtubule polymerization. The second class is microtubule-destabilizing agents which inhibit microtubule polymerization. The drugs of the latter class bind to the vinca or the colchicine binding site of tubulin (Botta et al., 2008; La Regina et al., 2019). It has been reported that inhibitors which interact with colchicine binding site have advantages over those targeting other binding sites, such as improved aqueous solubility, lower toxicity and multidrug resistance effects (Pettit et al., 1989, 1995; Stengel et al., 2010; Lu et al., 2012; Li et al., 2019) Many natural and synthetic 1,3-benzodioxole derivatives as podophyllotoxin (Desbène and Giorgi-Renault, 2002), steganacin (Lu et al., 2012), combretastatin A-2 (Pettit and Singh, 1987) as well as compounds **I** and **II** (Batra et al., 1985; Yi et al., 2012) (Fig. 1) possess anticancer activity with tubulin polymerization inhibitory effect through binding to colchicine binding site. Also, some 1,4-benzodioxine

* Corresponding author at: Medicinal and Pharmaceutical Chemistry Department, Pharmaceutical Chemistry Group, Pharmaceutical and Drug Industries Research Division, National Research Centre, 12622 Dokki, Giza, Egypt.
E-mail address: mnaboulenein@yahoo.com (M.N. Aboul-Enein).

https://doi.org/10.1016/j.ejps.2019.105045
Received 15 June 2019; Received in revised form 21 July 2019; Accepted 13 August 2019
Available online 14 August 2019
0928-0987/

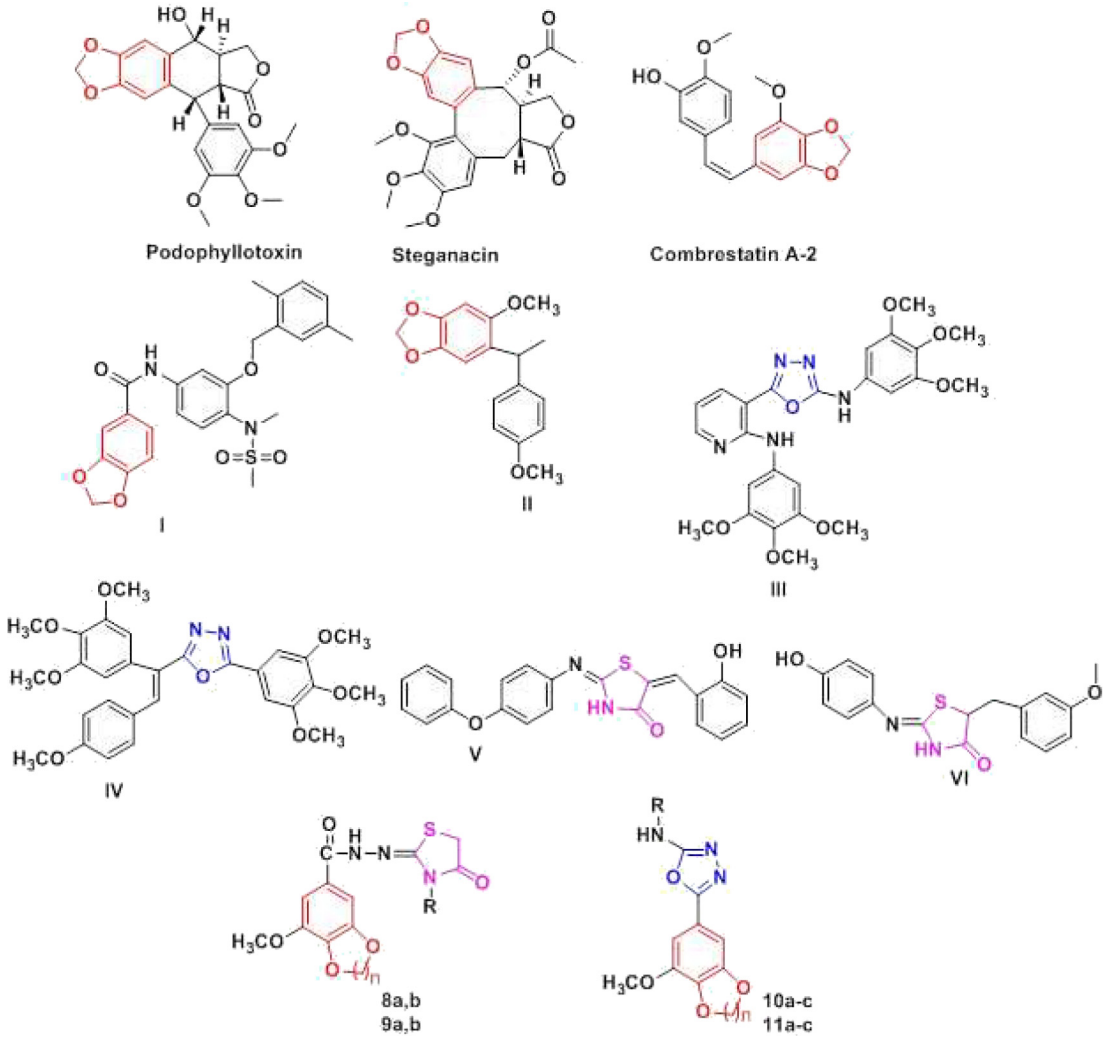

Fig. 1. Structures of some reported tubulin polymerization inhibitors and the target compounds **8a**, **b**, **9a**, **b**, **10a–c** and **11a–c** (Red: 1,3-benzodioxole, Blue: 1,3,4-oxadiazole and Magenta: thiazolidin-4-one). (For interpretation of the references to color in this figure legend, the reader is referred to the web version of this article.)

congeners have been reported to inhibit tubulin polymerization (Kiselyov et al., 2010).

On the other hand, 1,3,4-oxadiazoles possess various biological activities (Jayashankar et al., 2009; Rashid et al., 2012) due to presence of –N = C-O- linkage (Rigo and Couturier, 1985; Patel et al., 2013). Some of 1,3,4- oxadiazoles exhibited their anticancer activity through inhibition of tubulin polymerization such as compounds **III** (Kamal et al., 2011) and **IV** (Kamal et al., 2016). Also, certain thiazolidin-4-ones as compounds **V** (Zhang et al., 2013) and **VI** (Mu et al., 2015) have been reported to exhibit good tubulin polymerization inhibition activity (Fig. 1).

It is well known that hybridization of two or more bioactive scaffolds in a single compound is an reliable approach for developing of novel more effective bio-candidates (Aboul-Enein et al., 2015). With these aspects in mind, new hybrid structures of 1,3-benzodioxole and its higher homologue 1,4-benzodioxine with 1,3,4-oxadiazole or thiazolidin-4-one rings have been designed, synthesized and evaluated for their antiproliferative activity against HepG2, PC-3, MCF-7 and A549 human cancer cell lines. Furthermore, the effect of potent antiproliferative candidates on human normal cell was assessed to determine the selectivity of these compounds. Besides, the tubulin polymerization inhibition activity of the most active compound was determined to explore its mechanism of action. In addition, the influence of the most active compound on cell cycle progression was studied as well as its effect on the apoptosis regulatory molecules in the cells.

2. Experimental

2.1. Chemistry

All melting points were measured by the Electrothermal Capillary apparatus and were uncorrected. Infrared spectra were recorded as KBr pellets with [JASCO FT/IR-6100 spectrometer] and the values are characterized in cm^{-1}. ^{1}H NMR (400 MHz) and ^{13}C NMR (100 MHz) spectra were performed on [Jeol ECA 500 MHz spectrometer] and chemical shift values were recorded in ppm. Mass spectral data were measured with electron impact ionization technique at 70 eV. Elemental microanalyses were performed at Microanalytical Units in the National Research Centre as well as Cairo University. Column chromatography was done using silica gel as a stationary phase.

2.1.1. Synthesis of methyl 3,4,5-trihydroxybenzoate (2)

A solution of 17 g (0.1 mol) gallic acid and 0.002 g (0.01 mmol) of p-toluene sulfonic acid in 100 mL methanol was refluxed under stirring overnight. The mixture was cooled, the solvent was evaporated under vacuum and the residual was dissolved in EtOAc. Thereafter, the organic phase was shaken with 10% $NaHCO_3$ solution, dried (Na_2SO_4) and evaporated to obtain **2** in 75% yield as buff solid m.p. 198 °C [lit. (Mostafa et al., 2006) 200 °C].

*2.1.2. Synthesis of methyl 3,4-dihydroxy-5-methoxybenzoate (**3**)*

Methyl 3,4,5-trihydroxybenzoate (50 g, 270 mmol) (**2**) and borax (54 g, 140 mmol) were dissolved in distilled water (1 L) and stirred at room temperature for 1 h. A solution of 13% NaOH was added and the solution was stirred for 10 min followed by addition of dimethylsulfate (135 mL, 370 mmol) and further stirred for 15 h. The reaction was neutralized to pH 7–8 using 10% sulfuric acid, extracted with ethyl acetate, dried (Na_2SO_4) and evaporated *in vacuo* to afford compound **3** as a crude brown solid which was subjected to purification through column chromatography using petroleum ether (40–60): EtOAc 70:30 as mobile phase to obtain methyl 3,4-dihydroxy-5-methoxybenzoate (42.5 g, yield 79%) as a white solid m.p. 112 °C [lit. (Pettit and Singh, 1987) 110–111 °C].

*2.1.3. General procedure for synthesis of methyl 7-methoxybenzo[d][1,3] dioxole-5-carboxylate (**4a**) and methyl 8-methoxy-2,3-dihydrobenzo[b] [1,4]dioxine-6-carboxylate (**4b**)*

To 0.108 mol of dichloromethane or dichloroethane and 19.9 g (0.144 mol) of K_2CO_3 in 300 mL DMF, 14.4 g (0.0727 mol) of **3** in 250 mL DMF was added dropwise under stirring and the mixture was heated at 90 °C for 12 h. After cooling to room temperature, the reaction mixture was filtered and the remaining residue was washed with EtOAc. The filtrate was shaken with water, dried (Na_2SO_4) and evaporated. The obtained solid was column chromatographed using petroleum ether (40–60): EtOAc 60:40 as mobile phase to give the desired compounds.

4a: White solid, yield 65%, m.p. 92 °C [lit. (Zhang et al., 2007) 89–90 °C].
4b: White solid, yield 60%, m.p. 104 °C [lit. (Tsyganov et al., 2013) 106–108 °C].

*2.1.4. Synthesis of 7-methoxybenzo[d][1,3]dioxole-5-carbohydrazide (**5a**) and 8-methoxy-2,3-dihydrobenzo[b][1,4]dioxine-6-carbohydrazide (**5b**)*

A mixture of 5 mmol of methyl ester **4a** or **4b** and 25 mmol of hydrazine hydrate (98%) in 5 mL of methanol was refluxed for 6 h (to get **5a**) or 5 days (to get **5b**). After cooling a white precipitate of the desired hydrazide **5a** or **5b** was formed and filtered off.

5a: White solid, yield 85%, m.p. 204 °C [lit. (Semenov et al., 2010) 205–206 °C].
8-Methoxy-2,3-dihydrobenzo[b][1,4]dioxine-6-carbohydrazide (**5b**)

White solid, m.p. 178–180 °C, yield 80%; IR (KBr, cm^{-1}) 3436, 3298 (NH, NH_2), 1611 (C=O); ^{1}H NMR (DMSO d_6, δ, ppm): 3.89 (s, 3H, OCH_3), 4.20 (s, 4H, 2× $\underline{CH_2}$-benzdioxine), 4.39 (s, 2H, NH_2), 6.98–7.03 (m, 2H, $H_{ar.}$), 9.58 (s, 1H, NH); ^{13}C NMR (DMSO d_6, δ, ppm): 56.32 (OCH_3), 64.39, 64.511 (2× $\underline{CH_2}$-benzdioxine), 103.87, 109.27, 125.37, 136.05, 143.79, 148.88 (aromatic carbons), 165.84 (C=O); MS (EI) *m/z* (%): 224 (M^+, 14); Anal. calcd. for $C_{10}H_{12}N_2O_4$: C, 53. 57; H, 5.39; N, 12.49. Found: C, 53.71; H, 5.50; N, 12.32.

*2.1.5. General procedure for synthesis of N-alkyl/arayl-2-(7-methoxybenzo [d][1,3]dioxole-5-carbonyl)hydrazine-1-carbothioamide (**6a–e**) and 2-(8-methoxy-2,3-dihydrobenzo[b][1,4]dioxine-6-carbonyl)-N-alkyl/arayl hydrazine-1-carbothioamide (**7a–e**)*

The appropriate isothiocyanate (0.01 mol) was added to a stirred ethanolic solution of 0.01 mol of **5a** or **5b**. The reaction mixture was refluxed for 1 h. The obtained solid was filtered, washed with diethyl ether and dried.

*2.1.5.1. 2-(7-Methoxybenzo[d][1,3]dioxole-5-carbonyl)-N-methylhydrazine-1-carbothioamide (**6a**).* White solid, m.p. 224 °C, yield 93%; IR (KBr, cm^{-1}) 3702, 3687, 3440 (3NH), 1620 (C=O); ^{1}H NMR (DMSO d_6, δ, ppm): 2.96 (s, 3H, CH_3), 3.83 (s, 3H, OCH_3), 5.87 (s, 2H, $\underline{CH_2}$-benzodioxole), 7.12–7.23 (m, 2H, $H_{ar.}$), 7.99 (s, 1H, NH), 9.27 (s, 1H, NH), 10.18 (s, 1H, NH); ^{13}C NMR (DMSO d_6, δ, ppm): 31.4 (CH_3), 56.9 (OCH_3), 102.4 ($\underline{CH_2}$-benzodioxole), 102.6, 108.9, 127.1, 138.3, 143.2, 148.7 (aromatic carbons), 165.6 (C=O), 182.3 (C=S); MS (EI) *m/z* (%): 283 (M^+, 2.28), 179 (100); Anal. calcd. for $C_{11}H_{13}N_3O_4S$: C, 46.64; H, 4.63; N, 14.83; S, 11.32. Found: C, 46.82; H, 4.76; N, 14.95; S, 11.50.

*2.1.5.2. N-Butyl-2-(7-methoxybenzo[d][1,3]dioxole-5-carbonyl) hydrazine-1-carbothioamide (**6b**).* White solid, m.p. 210 °C, yield 88%; IR (KBr, cm^{-1}) 3436, 3316, 3265 (3NH), 1620 (C=O); ^{1}H NMR (DMSO d_6, δ, ppm): 0.82–0.85 (t, 3H, J = 7.65 Hz, $C\underline{H_3}$-CH_2-CH_2-CH_2-), 1.23 (m, 2H, CH_3-$\underline{CH_2}$-CH_2-CH_2-), 1.46 (s, 2H, CH_3-CH_2-$\underline{CH_2}$-CH_2-), 3.41–3.42 (t, 2H, J = 6.4 Hz, CH_3-CH_2-CH_2-$\underline{CH_2}$-), 3.86 (s, 3H, $OC\underline{H_3}$), 6.07 (s, 2H, $\underline{CH_2}$-benzodioxole), 7.14–7.25 (m, 2H, $H_{ar.}$), 8.04 (s, 1H, NH), 9.16 (s, 1H, NH) 10.19 (s, 1H, NH); ^{13}C NMR (DMSO d_6, δ, ppm): 14.3 ($C\underline{H_3}$-CH_2-CH_2-CH_2-), 19.9 (CH_3-$\underline{CH_2}$-CH_2-CH_2-), 31.3 (CH_3-CH_2-$\underline{CH_2}$-CH_2-), 43.8 (CH_3-CH_2-CH_2-$\underline{CH_2}$-), 56.9 (OCH_3), 102.4 ($\underline{CH_2}$-benzodioxole), 102.6, 109.1, 127.1, 138.3, 143.2, 148.7 (aromatic carbons), 165.5 (C=O), 181.8 (C=S); MS (EI) *m/z* (%): 324 (M^+, 2.1); Anal. calcd. for $C_{14}H_{19}N_3O_4S$: C, 51.68; H, 5.89; N, 12.91; S, 9.85. Found: C, 51.76; H, 5.98; N, 13.12; S, 9.99.

*2.1.5.3. 2-(7-Methoxybenzo[d][1,3]dioxole-5-carbonyl)-N-phenylhydrazine-1-carbothioamide (**6c**).* White solid, m.p. 218 °C, yield 87%; IR (KBr, cm^{-1}) 3312, 3277, 3218 (3NH), 1617 (C=O); ^{1}H NMR (DMSO d_6, δ, ppm): 3.84 (s, 3H, OCH_3), 6.06 (s, 2H, $\underline{CH_2}$-benzodioxole), 7.12–7.29 (m, 7H, $H_{ar.}$), 9.67–9.74 (m, 2H, 2NH), 10.38 (s, 1H, NH); ^{13}C NMR (DMSO d_6, δ, ppm): 56.9 (OCH_3), 102.6 ($\underline{CH_2}$-benzodioxole), 109.0, 125.6, 126.6, 127.2, 128.4, 138.4, 139.7, 143.3, 148.7 (aromatic carbons), 165.6 (C=O), 181.5 (C=S); MS (EI) *m/z* (%): 345 (M^+, 0.2), 179 (100); Anal. calcd. for $C_{16}H_{15}N_3O_4S$: C, 55.64; H, 4.38; N, 12.17; S, 9.28. Found: C, 55.82; H, 4.59; N, 12.25; S, 9.35.

*2.1.5.4. N-(4-Chlorophenyl)-2-(7-methoxybenzo[d][1,3]dioxole-5-carbonyl)hydrazine-1-carbothioamide (**6d**).* White solid, m.p. 208 °C, yield 90%; IR (KBr, cm^{-1}) 3439, 3315, 3223 (3NH), 1617 (C=O); ^{1}H NMR (DMSO d_6, δ, ppm): 3.87 (s, 3H, OCH_3), 6.07 (s, 2H, $\underline{CH_2}$-benzodioxole), 7.18–7.38 (m, 6H, $H_{ar.}$), 9.77 (s, 1H, NH), 9.82 (s, 1H, NH), 10.45 (s, 1H, NH); ^{13}C NMR (DMSO d_6, δ, ppm): 56.9 (OCH_3), 102.4 ($\underline{CH_2}$-benzodioxole), 102.9, 109.0, 127.0, 128.0, 128.3, 129.4, 138.4, 138.7, 143.3, 148.7 (aromatic carbons), 165.5 (C=O), 182.2 (C=S); MS (EI) *m/z* (%): 379.8 (M^+, 8); Anal. calcd. for $C_{16}H_{14}ClN_3O_4S$: C, 50.60; H, 3.72; N, 11.06; S, 8.44. Found: C, 50.82; H, 3.91; N, 11.19; S, 8.65.

*2.1.5.5. 2-(7-Methoxybenzo[d][1,3]dioxole-5-carbonyl)-N-(4-methoxyphenyl)hydrazine-1-carbothioamide (**6e**).* White solid, m.p. 210 °C, yield 90%; IR (KBr, cm^{-1}) 3750, 3447, 3314 (3NH), 1622 (C=O); ^{1}H NMR (DMSO d_6, δ, ppm): 3.75 (s, 3H, OCH_3), 3.89 (s, 3H, OCH_3), 6.10 (s, 2H, $\underline{CH_2}$-benzodioxole), 6.89–6.91 (m, 2H, $H_{ar.}$), 7.22–7.32 (m, 4H, $H_{ar.}$), 9.58 (s, 1H, NH), 9.67 (s, 1H, NH), 10.38 (s, 1H, NH); ^{13}C NMR (DMSO d_6, δ, ppm): 55.6, 56.9 (2× OCH_3), 102.4 ($\underline{CH_2}$-benzodioxole), 102.8, 109.0, 113.7, 127.0, 128.0, 132.3, 138.3, 143.2, 148.6, 157.2 (aromatic carbons), 165.6 (C=O), 181.9 (C=S); MS (EI) *m/z* (%): 375.8 (M^+, 21); Anal. calcd. for $C_{17}H_{17}N_3O_5S$: C, 54.39; H, 4.56; N, 11.19; S, 8.54. Found: C, 54.49; H, 4.65; N, 11.28; S, 8.75.

*2.1.5.6. 2-(8-Methoxy-2,3-dihydrobenzo[b][1,4]dioxine-6-carbonyl)-N-methylhydrazine-1-carbothioamide (**7a**).* White solid, m.p. 232 °C, yield 94%; IR (KBr, cm^{-1}) 3438, 3289, 3229 (3NH), 1667 (C=O); ^{1}H NMR (DMSO d_6, δ, ppm): 2.86 (s, 3H, CH_3), 3.80 (s, 3H, OCH_3), 4.24–4.29 (m, 4H, 2× $\underline{CH_2}$-benzodioxine),7.13–7.14 (m, 2H, H_{ar}), 8.00 (s, 1H, NH), 9.26 (s, 1H, NH), 10.16 (s, 1H, NH); ^{13}C NMR (DMSO d_6, δ, ppm): 30.9 (CH_3), 55.9 (OCH_3), 63.9, 64.1 (2× $\underline{CH_2}$-benzodioxine), 104.2,

109.8, 123.9, 136.1, 143.1, 148.3 (aromatic carbons), 165.2 (C=O), 182.1 (C=S); MS (EI) *m/z* (%): 297 (M^+, 0.16); Anal. calcd. for $C_{12}H_{15}N_3O_4S$: C, 48.48; H, 5.09; N, 14.13; S, 10.78. Found: C, 48.67; H, 5.18; N, 14.24; S, 10.97.

*2.1.5.7. N-butyl-2-(8-methoxy-2,3-dihydrobenzo[b][1,4]dioxine-6-carbonyl)hydrazine-1-carbothioamide (**7b**)*. White solid, m.p. 200 °C, yield 90%; IR (KBr, cm^{-1}) 3746, 3442, 3279 (3NH), 1664 (C=O); ^{1}H NMR (DMSO d_6, δ, ppm): 0.82–0.85 (t, 3H, J = 7.65 Hz, C<u>H</u>$_3$-CH$_2$-CH$_2$-CH$_2$-), 1.25 (m, 2H, CH$_3$-<u>CH$_2$</u>-CH$_2$-CH$_2$-),1.46 (s, 2H, CH$_3$-CH$_2$-<u>CH$_2$</u>-CH$_2$-), 3.41–3.42 (t, 2H, J = 6 Hz, CH$_3$-CH$_2$-CH$_2$-<u>CH$_2$</u>-), 3.79 (s, 3H, OCH$_3$), 4.24–4.25 (m, 4H, 2× <u>CH$_2$</u>-benzodioxine), 7.11–7.13 (m, 2H, H$_{ar.}$), 8.01 (s, 1H, NH), 9.13 (s, 1H, NH), 10.16 (s, 1H, NH); ^{13}C NMR (DMSO d_6, δ, ppm): 14.2 (C<u>H</u>$_3$-CH$_2$-CH$_2$-CH$_2$-), 19.8 (CH$_3$-<u>CH$_2$</u>-CH$_2$-CH$_2$-), 31.3 (CH$_3$-CH$_2$-<u>CH$_2$</u>-CH$_2$-), 43.8 (CH$_3$-CH$_2$-CH$_2$-<u>CH$_2$</u>-), 56.3 (OCH$_3$), 64.3, 64.5 (2× CH$_2$, <u>CH$_2$</u>-benzodioxine), 104.5, 110.2, 124.2, 136.6, 143.6, 148.7 (aromatic carbons), 165.9 (C=O), 184.2 (C=S); MS (EI) *m/z* (%): 339 (M^+, 100); Anal. calcd. for $C_{15}H_{21}N_3O_4S$: C, 53.08; H, 6.24; N, 12.38; S, 9.45. Found: C, 53.26; H, 6.35; N, 12.45; S, 9.67.

*2.1.5.8. 2-(8-Methoxy-2,3-dihydrobenzo[b][1,4]dioxine-6-carbonyl)-N-phenylhydrazine-1-carbothioamide (**7c**)*. White solid, m.p. 194 °C, yield 92%; IR (KBr, cm^{-1}) 3439, 3300, 3167 (3NH), 1630 (C=O); ^{1}H NMR (DMSO d_6, δ, ppm): 3.88 (s, 3H, OCH$_3$), 4.24–4.25 (m, 4H, 2× <u>CH$_2$</u>-benzodioxine), 7.09–7.32 (m, 7H, H$_{ar.}$), 8.01 (s, 1H, NH), 9.15 (s, 1H, NH), 9.63 (s, 1H, NH); ^{13}C NMR (DMSO d_6, δ, ppm): 56.2 (OCH$_3$), 64.3, 64.4 (2× CH$_2$, <u>CH$_2$</u>-benzodioxine), 103.8, 109.2, 123.9, 124.5, 125.3, 128.5, 136.0, 139.7, 143.7, 148.8 (aromatic carbons), 165.8 (C=O), 179.8 (C=S); MS (EI) *m/z* (%): 360 (M^+ +1, 35); Anal. calcd. for $C_{17}H_{17}N_3O_4S$: C, 56.81; H, 4.77; N, 11.69; S, 8.92. Found: C, 56.92; H, 4.86; N, 11.80; S, 9.13.

*2.1.5.9. N-(4-chlorophenyl)-2-(8-methoxy-2,3-dihydrobenzo[b][1,4]dioxine-6-carbonyl)hydrazine-1-carbothioamide (**7d**)*. White solid, m.p. 218 °C, yield 91%; IR (KBr, cm^{-1}) 3884, 3746, 3295 (3NH), 1670 (C=O); ^{1}H NMR (DMSO d_6, δ, ppm): 3.80 (s, 3H, OCH$_3$), 4.25–4.26 (m, 4H, 2× <u>CH$_2$</u>-benzodioxine), 7.16–7.17 (m, 2H, H$_{ar.}$), 7.36–7.45 (m, 4H, H$_{ar.}$), 9.76 (s, 1H, NH), 9.82 (s, 1H, NH), 10.43 (s, 1H, NH); ^{13}C NMR (DMSO d_6, δ, ppm): 56.3 (OCH$_3$), 64.3, 64.6 (2× CH$_2$, <u>CH$_2$</u>-benzodioxine), 104.6, 110.3, 118.2, 124.1, 128.3, 129.7, 136.7, 138.5, 143.6, 148.7 (aromatic carbons), 166.0 (C=O), 183.2 (C=S); MS (EI) *m/z* (%): 392.8 (M^+, 3); Anal. calcd. for $C_{17}H_{16}ClN_3O_4S$: C, 51.84; H, 4.10; N, 10.67; S, 8.14. Found: C, 51.98; H, 4.32; N, 10.78; S, 8.25.

*2.1.5.10. 2-(8-Methoxy-2,3-dihydrobenzo[b][1,4]dioxine-6-carbonyl)-N-(4-methoxyphenyl)hydrazine-1-carbothioamide (**7e**)*. White solid, m.p. 185 °C, yield 90%; IR (KBr, cm^{-1}) 3884, 3746, 3295 (3NH), 1670 (C=O); ^{1}H NMR (DMSO d_6, δ, ppm): 3.75 (s, 3H, OCH$_3$), 3.82 (s, 3H, OCH$_3$), 4.27–4.28 (m, 4H, 2× <u>CH$_2$</u>-benzodioxine), 6.89–6.91 (m, 2H, H$_{ar.}$), 7.19–7.30 (m, 4H, H$_{ar.}$), 9.57 (s, 1H, NH), 9.67 (s, 1H, NH), 10.35 (s, 1H, NH); ^{13}C NMR (DMSO d_6, δ, ppm): 55.67, 56.3 (2× OCH$_3$), 64.3, 69.9 (2× CH$_2$, <u>CH$_2$</u>-benzodioxine), 104.7, 110.4, 113.6, 124.4, 128.0, 132.5, 136.6, 143.6, 148.7, 157.2 (aromatic carbons), 165.8 (C=O), 182.2 (C=S); MS (EI) *m/z* (%): 388.4 (M^+, 16); Anal. calcd. for $C_{18}H_{19}N_3O_5S$: C, 55.52; H, 4.92; N, 10.79; S, 8.23. Found: C, 55.71; H, 5.14; N, 10.87; S, 8.44.

*2.1.6. General method for synthesis of 7-methoxy-N′-(3-alkyl-4-oxothiazolidin-2-ylidene)benzo[d][1,3]dioxole-5-carbohydrazide (**8a, b**),8-methoxy-N′-(3-alkyl-4-oxothiazolidin-2-ylidene)-2,3-dihydrobenzo[b][1,4]dioxine-6-carbohydrazide (**9a, b**), N-aryl-5-(7-methoxybenzo[d][1,3]dioxol-5-yl)-1,3,4-oxadiazol-2-amine (**10a–c**) and N-4-aryl-5-(8-methoxy-2,3-dihydrobenzo[b][1,4]dioxin-6-yl)-1,3,4-oxadiazol-2-amine (**11a–c**)*

To 0.0035 mol of **6a–e** or **7a–e** in absolute ethanol (30 mL), ethyl bromoacetate (0.0055 mol) and anhydrous sodium acetate (0.04 mol) were added and the mixture was refluxed while stirring for 5 h. Thereafter, the mixture was evaporated *in vacuo*, the crude product was column chromatographed using a mixture of DCM:EtOAC (7:3) as a mobile phase to give the desired compounds.

*2.1.6.1. 7-Methoxy-N′-(3-methyl-4-oxothiazolidin-2-ylidene)benzo[d][1,3]dioxole-5-carbohydrazide (**8a**)*. Yellowish white solid, m.p. 198 °C, yield 75%; IR (KBr, cm^{-1}) 3426 (NH), 1719, 1622 (2 C=O); ^{1}H NMR (DMSO d_6, δ, ppm): 3.15 (s, 3H, CH$_3$), 3.86 (s, 3H, OCH$_3$), 4.00 (s, 2H, <u>CH$_2$</u>-thiazolidine), 6.07 (s, 2H, <u>CH$_2$</u>-benzodioxole), 7.06–7.18 (m, 2H, H$_{ar.}$), 10.78 (s, 1H, NH); ^{13}C NMR (DMSO d_6, δ, ppm): 29.7 (CH$_2$, <u>CH$_2$</u>-thiazolidine), 33.0 (CH$_3$), 56.9 (OCH$_3$), 101.7 (CH$_2$, <u>CH$_2$</u>-benzodioxole), 102.5, 108.5, 127.7, 138.0, 143.3, 148.7 (aromatic carbons), 162.8, 163.9, 172.3 (C=N, 2× C=O); MS (EI) *m/z* (%): 323 (M^+, 100); Anal. calcd. for $C_{13}H_{13}N_3O_5S$: C, 48.29; H, 4.05; N, 13.00; S, 9.92. Found: C, 48.21; H, 3.91; N, 12.88; S, 9.71.

*2.1.6.2. N′-(3-butyl-4-oxothiazolidin-2-ylidene)-7-methoxybenzo[d][1,3]dioxole-5-carbohydrazide (**8b**)*. Yellowish white solid, m.p. 204 °C, yield 78%; IR (KBr, cm^{-1}) 3211 (NH), 1736, 1621 (2 C=O); ^{1}H NMR ($CDCl_3$, δ, ppm): 0.89–92 (t, *J* = 6.7 Hz, 3H, C<u>H</u>$_3$-CH$_2$-CH$_2$-CH$_2$-), 1.32 (m, 2H, CH$_3$-<u>CH$_2$</u>-CH$_2$-CH$_2$-), 1.64 (m, 2H, CH$_3$-CH$_2$-<u>CH$_2$</u>-CH$_2$-), 3.79–3.83 (m, 4H, CH$_3$-CH$_2$-CH$_2$-<u>CH$_2$</u>-, <u>CH$_2$</u>-thiazolidine), 3.91 (s, 3H, OCH$_3$), 6.02 (s, 2H, <u>CH$_2$</u>-benzodioxole), 7.13–7.33 (m, 2H, H$_{ar.}$), 8.21 (s, 1H, NH); ^{13}C NMR (DMSO d_6, δ, ppm): 13.7 (C<u>H</u>$_3$-CH$_2$-CH$_2$-CH$_2$-), 20.0 (CH$_3$-<u>CH$_2$</u>-CH$_2$-CH$_2$-), 29.1 (CH$_3$-CH$_2$-<u>CH$_2$</u>-CH$_2$-), 32.9 (CH$_2$, <u>CH$_2$</u>-thiazolidine), 43.5 (CH$_3$-CH$_2$-CH$_2$-<u>CH$_2$</u>-), 56.9 (OCH$_3$), 101 (CH$_2$, <u>CH$_2$</u>-benzodioxole), 102.3, 108.4, 127.2, 138.5, 143.7, 148.9 (aromatic carbons), 159.6, 163.9, 170.8 (C=N, 2× C=O); MS (EI) *m/z* (%): 365 (M^+, 100); Anal. calcd. for $C_{16}H_{19}N_3O_5S$: C, 52.59; H, 5.59; N, 11.50; S, 8.77. Found: C, 52.57; H, 5.60; N, 11.52; S, 8.79.

*2.1.6.3. 8-Methoxy-N′-(3-methyl-4-oxothiazolidin-2-ylidene)-2,3-dihydrobenzo[b][1,4]dioxine-6-carbohydrazide (**9a**)*. Yellowish white solid, m.p. 218 °C, yield 78%; IR (KBr, cm^{-1}) 3434 (NH), 1716, 1629 (2 C=O); ^{1}H NMR (DMSO d_6, δ, ppm): 2.96 (s, 3H, CH$_3$), 3.83 (s, 3H, OCH$_3$), 4.00 (s, 2H, <u>CH$_2$</u>-thiazolidine), 4.22 (s, 4H, 2× <u>CH$_2$</u>-benzodioxine), 6.90–7.03 (m, 2H, H$_{ar.}$), 10.64 (s, 1H, NH); ^{13}C NMR (DMSO d_6, δ, ppm): 29.7 (CH$_2$, <u>CH$_2$</u>-thiazolidine), 32.1 (CH$_3$), 56.3 (OCH$_3$), 64.4, 64.5 (2× CH$_2$, <u>CH$_2$</u>-benzodioxine), 104.2, 109.7, 126.9, 125.4, 136.4, 143.7, 148.9 (aromatic carbons) 163.0, 163.7, 172.2 (C=N, 2× C=O); MS (EI) *m/z* (%): 336.9 (M^+, 100); Anal. calcd. for $C_{14}H_{15}N_3O_5S$: C, 49.85; H, 4.48; N, 12.46; S, 9.50. Found: C, 49.96; H, 4.67; N, 12.65; S, 9.71.

*2.1.6.4. N′-(3-butyl-4-oxothiazolidin-2-ylidene)-8-methoxy-2,3-dihydrobenzo[b][1,4]dioxine-6-carbohydrazide (**9b**)*. Yellowish white solid, m.p. 224 °C, yield 72%; IR (KBr, cm^{-1}) 3437 (NH), 1719, 1645 (2 C=O); ^{1}H NMR ($CDCl_3$, δ, ppm): 0.89–0.91 (t, *J* = 6.7 Hz, 3H, C<u>H</u>$_3$), 1.22–1.32 (m, 2H, CH$_3$-<u>CH$_2$</u>-CH$_2$-CH$_2$-), 1.64–1.66 (m, 2H, CH$_3$-CH$_2$-<u>CH$_2$</u>-CH$_2$-), 3.79–3.89 (m, 4H, CH$_3$-CH$_2$-CH$_2$-<u>CH$_2$</u>-, <u>CH$_2$</u>-thiazolidine), 3.93 (s, 3H, OCH$_3$), 4.25–4.33 (m, 4H, 2× <u>CH$_2$</u>-benzodioxine), 6.94–7.25 (m, 2H, H$_{ar.}$), 8.20 (s, 1H, NH); ^{13}C NMR (DMSO d_6, δ, ppm): 13.7 (C<u>H</u>$_3$-CH$_2$-CH$_2$-CH$_2$-), 20.0 (CH$_3$-<u>CH$_2$</u>-CH$_2$-CH$_2$-), 29.1 (CH$_3$-CH$_2$-<u>CH$_2$</u>-CH$_2$-), 32.9 (CH$_2$, <u>CH$_2$</u>-thiazolidine), 43.5 (CH$_3$-CH$_2$-CH$_2$-<u>CH$_2$</u>-), 56.4 (OCH$_3$), 64.2, 64.8 (2× CH$_2$, <u>CH$_2$</u>-benzodioxine), 104.1, 108.6, 125.0, 136.5, 143.6, 149.2 (aromatic carbons), 159.1, 164.0, 170.8 (C=N, 2× C=O); MS (EI) *m/z* (%): 379 (M^+, 60); Anal. calcd. for $C_{17}H_{21}N_3O_5S$: C, 53.81; H, 5.58; N, 11.07; S, 8.45. Found: C, 54.10; H, 5.67; N, 11.19; S, 8.66.

*2.1.6.5. 5-(7-Methoxybenzo[d][1,3]dioxol-5-yl)-N-phenyl-1,3,4-oxadiazol-2-amine (**10a**)*. White solid, m.p. 230 °C, yield 87%; IR (KBr, cm^{-1}) 3427 (NH); ^{1}H NMR (DMSO d_6, δ, ppm): 3.87 (s, 3H, OCH$_3$), 6.09 (s, 2H, <u>CH$_2$</u>-benzodioxole), 6.97–7.10 (m, 3H, H$_{ar.}$), 7.32 (m, 2H,

$H_{ar.}$), 7.56 (m, 2H, $H_{ar.}$); ^{13}C NMR (DMSO d_6, δ, ppm): 56.8 (OCH_3), 100 (CH_2, $\underline{CH_2}$-benzodioxole), 102.7, 106.1, 117.5, 118.3, 122.3, 129.5, 137.7, 139.2, 144.1, 149.5 (aromatic carbons), 157.9, 160.1 (2× C═N); MS (EI) *m/z* (%): 311(M^+, 53); Anal. calcd. for $C_{16}H_{13}N_3O_4$: C, 61.73; H, 4.21; N, 13.50. Found: C, 61.95; H, 4.42; N, 13.71.

*2.1.6.6. N-(4-chlorophenyl)-5-(7-methoxybenzo[d][1,3]dioxol-5-yl)-1,3,4-oxadiazol-2-amine (**10b**).* White solid, m.p. 230 °C, yield 82%; IR (KBr, cm^{-1}) 3437 (NH); ^{1}H NMR (DMSO d_6, δ, ppm): 3.80 (s, 3H, OCH_3), 6.08 (s, 2H, $\underline{CH_2}$-benzodioxole), 7.02–7.09 (m, 2H, $H_{ar.}$), 7.36 (d, 2H, J = 8.6 Hz, $H_{ar.}$), 7.58 (d, 2H, J = 8.6, $H_{ar.}$); ^{13}C NMR (DMSO d_6, δ, ppm): 56.8 (OCH_3), 100.4 (CH_2, $\underline{CH_2}$-benzodioxole), 102.6, 106.01, 118.3, 119.0, 125.6, 129.5, 137.7, 138.3, 144.0, 149.4 (aromatic carbons), 157.5, 159.5 (2× C═N); MS (EI) *m/z* (%): 344.97 (M^+, 100); Anal. calcd. for $C_{16}H_{12}ClN_3O_4$: C, 55.58; H, 3.50; N, 12.15. Found: C, 55.79; H, 3.71; N, 12.27.

*2.1.6.7. 5-(7-Methoxybenzo[d][1,3]dioxol-5-yl)-N-(4-methoxyphenyl)-2,5-dihydro-1,3,4-oxadiazol-2-amine (**10c**).* White solid, m.p. 210 °C, yield 85%; IR (KBr, cm^{-1}) 3423 (NH); ^{1}H NMR (DMSO d_6, δ, ppm): 3.73 (s, 3H, OCH_3), 3.90 (s, 3H, OCH_3), 6.11 (s, 2H, $\underline{CH_2}$-benzodioxole), 6.93–6.95 (d, 2H, J = 7.9 Hz, $H_{ar.}$), 7.02–7.1 (m, 2H, $H_{ar.}$), 7.52–7.54 (d, 2H, J = 7.9 Hz, $H_{ar.}$), 10.39 (s, 1H, NH); ^{13}C NMR (DMSO d_6, δ, ppm): 55.5, 56.7 (2× OCH_3), 99.9 (CH_2, $\underline{CH_2}$-benzodioxole), 102.6, 106, 114.7, 118.4, 118.8, 132.3, 137.6, 144.6, 149.4, 154.0 (aromatic carbons), 157.7, 160.2 (2×C═N); MS (EI) *m/z* (%): 341(M^+, 100); Anal. calcd. for $C_{17}H_{15}N_3O_5$: C, 59.82; H, 4.43; N, 12.31. Found: C, 59.91; H, 4.64; N, 12.53.

*2.1.6.8. 5-(8-Methoxy-2,3-dihydrobenzo[b][1,4]dioxin-6-yl)-N-phenyl-1,3,4-oxadiazol-2-amine (**11a**).* White solid, m.p. 198 °C, yield 79%; IR (KBr, cm^{-1}) 3432 (NH); ^{1}H NMR (DMSO d_6, δ, ppm): 3.80 (s, 3H, OCH_3), 4.26 (s, 4H, 2× $\underline{CH_2}$-benzodioxine), 6.93–7.01 (m, 2H, $H_{ar.}$), 7.31–7.58 (m, 4H, $H_{ar.}$); ^{13}C NMR (DMSO d_6, δ, ppm): 56.4 (OCH_3), 64.4, 64.6 (2× CH_2, $\underline{CH_2}$-benzodioxine), 102.2, 107.7, 116.1, 117.5, 122.1, 125.91, 129.5, 136.0, 139.4, 144.5, 149.7 (aromatic carbons), 157.9, 160.2 (2× C═N); MS (EI) *m/z* (%): 324.99 (M^+, 100); Anal. calcd. for $C_{17}H_{15}N_3O_4$: C, 62.76; H, 4.65; N, 12.92. Found: C, 62.97; H, 4.86; N, 13.11.

*2.1.6.9. N-(4-chlorophenyl)-5-(8-methoxy-2,3-dihydrobenzo[b][1,4]dioxin-6-yl)-1,3,4-oxadiazol-2-amine (**11b**).* White solid, m.p. 248 °C, yield 80%; IR (KBr, cm^{-1}) 3440 (NH); ^{1}H NMR (DMSO d_6, δ, ppm): 3.80 (s, 3H, OCH_3), 4.26 (s, 4H, 2× CH_2, $\underline{CH_2}$-benzodioxine), 6.93–700 (m, 1H, $H_{ar.}$), 7.38 (d, 2H, J = 8.6 Hz, $H_{ar.}$), 7.58 (d, 2H, J = 8.6 Hz, $H_{ar.}$), 10.77 (s, 1H, NH); ^{13}C NMR (DMSO d_6, δ, ppm): 56.4 (OCH_3), 64.5 (2× CH_2, $\underline{CH_2}$-benzodioxine), 102.2, 107.4, 116.0, 119, 125.91, 129.46, 136.15, 138.23, 144.5, 149.78 (aromatic carbons), 158.2, 159.9 (2× C═N); MS (EI) *m/z* (%): 358.88 (M^+, 100); Anal. calcd. for $C_{17}H_{14}ClN_3O_4$: C, 56.76; H, 3.92; N, 11.68. Found: C, 56.87; H, 4.14; N, 11.87.

*2.1.6.10. 5-(8-Methoxy-2,3-dihydrobenzo[b][1,4]dioxin-6-yl)-N-(4-methoxyphenyl)-2,5-dihydro-1,3,4-oxadiazol-2-amine (**11c**).* White solid, m.p. 214 °C, yield 82%; IR (KBr, cm^{-1}) 3440 (NH); ^{1}H NMR (DMSO d_6, δ, ppm): 3.73 (s, 3H, OCH_3), 3.85 (s, 3H, OCH_3), 4.30 (s, 4H, 2× CH_2, $\underline{CH_2}$-benzodioxine), 6.94–7.04 (m, 4H, $H_{ar.}$), 7.52–7.54 (d, 2H, J = 8 Hz, $H_{ar.}$), 10.49 (s, 1H, NH); ^{13}C NMR (DMSO d_6, δ, ppm): 55.6, 56.3 (2× OCH_3), 64.4, 64.5 (2× CH_2, $\underline{CH_2}$-benzodioxine), 102.0, 107.5, 114.7, 116.1, 118.9, 132.4, 135.8, 144.4, 149.6, 154.8 (aromatic carbons), 157.7, 160.3 (2× C═N); MS (EI) *m/z* (%): 355 (M^+, 100); Anal. calcd. for $C_{18}H_{17}N_3O_5$: C, 60.84; H, 4.82; N, 11.83. Found: C, 61.05; H, 4.93; N, 12.07.

2.2. Single-crystal X-ray study

A suitable crystal of compound **10a** for single crystal X-ray measurements was obtained through crystallization of an ethanolic solution of the compound. The data were collected at T = 298 K on Enraf Nonius 590 Kappa CCD single crystal diffractometer equipped with graphite monochromated MoKα (λ = 0.71073 Å) radiation using ψ–ω scan technique at room temperature. The crystal structure was determined by direct method using SIR92, SUPERFLIP, SHELXS (Altomare et al., 1994; Palatinus and Chapuis, 2007; Sheldrick, 2008) which revealed the positions of all non-hydrogen atoms then refined by the full matrix least squares refinement based on F^2 using maXus package (Mackay et al., 1999).

2.3. Biological evaluation

2.3.1. Cell lines and cell culture

Human HepG2, PC-3, MCF-7 as well as A549 carcinoma cell lines were purchased VACSERA-EGYPT. HepG2, PC3 and A549 cells were kept in RPMI-1640 medium [Biowest] whereas MCF-7 was cultured in [DMEM-F12 (Gibco)]. Media was augmented with 10% (v/v) fetal bovine serum (FBS; Gibco) and 1% Penicillin/Streptomycin (Sigma). Cells were protected at 37 °C in tissue culture flasks with 5% CO_2 completely humidified incubator.

2.3.2. In vitro cytotoxic assay

The target compounds were evaluated for their antiproliferative activity against panel of cell lines HepG2, PC-3, MCF-7 and A549 human carcinoma cell lines using colorimetric MTT [3-(4,5-dimethylthiazol-2-yl)-2,5-diphenyltetrazolium bromide] assay (Mosmann, 1983). Concisely, cells were sowed at density of 1×10^4 cells/well in a 96 well flat bottom plate. Media was aspirated then 180 µL fresh medium was added to the cells. After that, the compounds under investigation were added in triplicate to the wells at a range of concentrations (100, 50, 25, 12.5 µM). Wells which were treated with 0.5% DMSO was used as negative control while cells incubated with doxorubicin was used as positive control. The medium was detached and exchanged with 50 µL MTT solution [0.5 mg/mL; Sigma] after 48 h which is freshly diluted from a 5 mg/mL stock solution and the plates were incubated for 4 h at 37 °C till crystals became observable. After that 200 µL of 10% sodium dodecyl sulfate in deionized water was added for each well for discontinuation of the reaction and dissolving the formed crystals. Graph-Pad PRISM version-5 software was used to determine the IC_{50}.

2.3.3. In vitro cytotoxicity on human normal skin fibroblast cell line BJ1

Compound **11a** was evaluated on human normal skin fibroblast cell line BJ1 (ATCC number CRL-2522) for their cytotoxic effect using the same mentioned MTT assay protocol (Mosmann, 1983).

2.3.4. Cell cycle analysis

The MCF-7 cells (2×10^5/well) were incubated with compound **11a** at its IC_{50}. After 24 h ice-cold PBS was used to for washing the cells twice then the cells were collected and fixed ice-cold ethanol 70% (v/v) ethanol. The cells were washed again with PBS followed by re-suspending with [0.1 mg/mL RNase], staining with [40 mg/mL PI] and examination using flow cytometry [FACScalibur (Becton Dickinson)].

2.3.5. Tubulin polymerization assay

MCF-7 cells were cultured with DMEM and augmented with [10% FBS and 1% penicillin-streptomycin]. Plate cells with volume of 100 µL, complete growth medium and 100 µL of the tested compound per well were prepared in a 96-well plate for 18–24 h before the enzyme assay for tubulin. The microtiter plate which was used for this kit was pre-coated with specific antibody to TUBb. Then standards or samples were added to the suitable microtiter plate wells having a biotin-conjugated

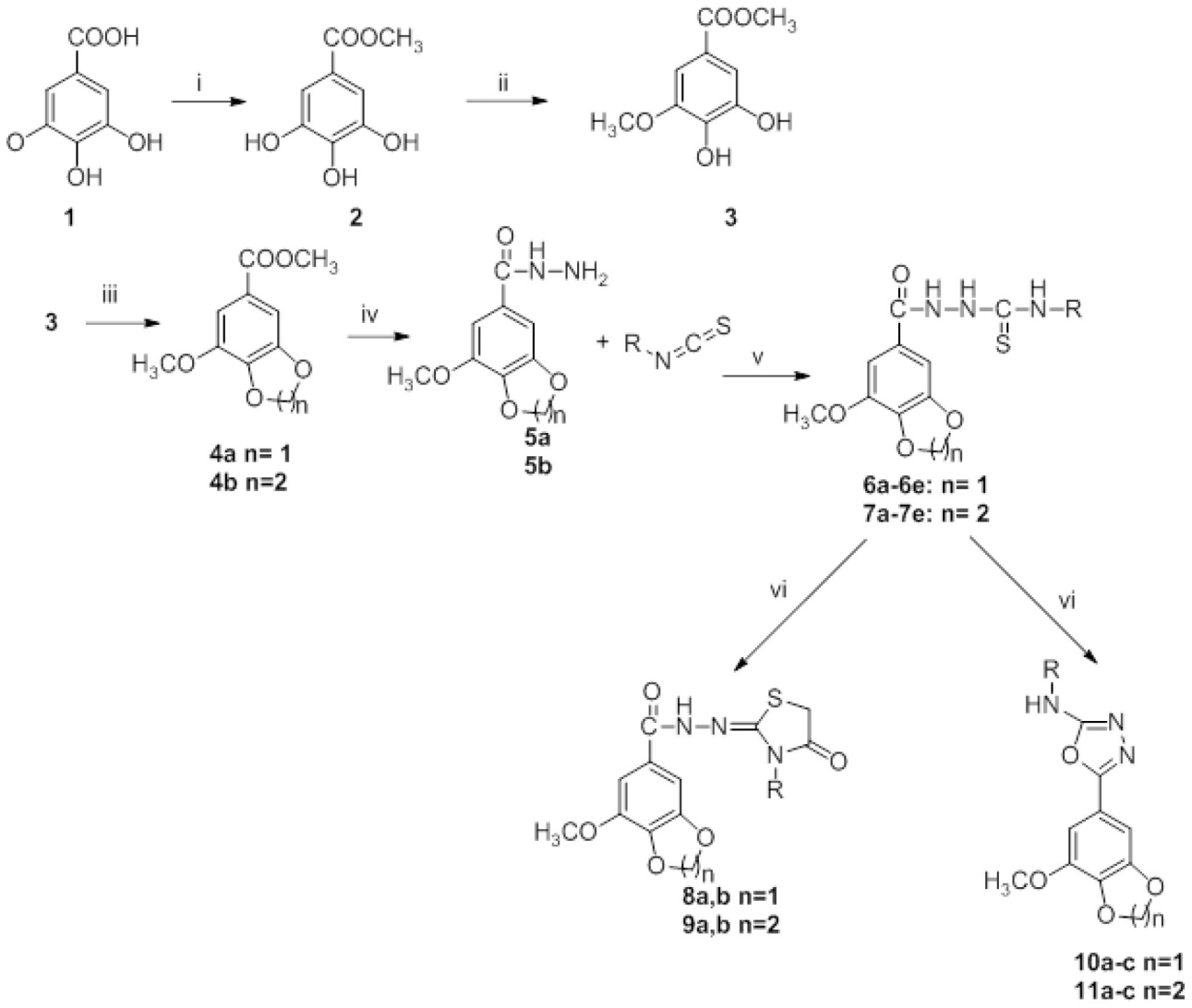

Compd No.	n	R	Compd No.	n	R
6a	1	Methyl	**8a**	1	Methyl
6b	1	n-Butyl	**8b**	1	n-Butyl
6c	1	C_6H_5-	**9a**	2	Methyl
6d	1	p-C_6H_4-Cl	**9b**	2	n-Butyl
6e	1	p-C_6H_4-OCH_3	**10a**	1	C_6H_5-
7a	2	Methyl	**10b**	1	p-C_6H_4-Cl
7b	2	n-Butyl	**10c**	1	p-C_6H_4-OCH_3
7c	2	C_6H_5-	**11a**	2	C_6H_5-
7d	2	p-C_6H_4-Cl	**11b**	2	p-C_6H_4-Cl
7e	2	p-C_6H_4-OCH_3	**11c**	2	p-C_6H_4-OCH_3

Scheme 1. Synthesis of target compounds **8a–b**, **9a–b**, **10a–c** and **11a–c**.
Reagents and conditions: i) PTSA, MeOH, reflux, overnight. ii) Borax, NaOH, dimethyl sulfate, r.t. 15 h. iii): CH_2Cl_2 or $ClCH_2CH_2Cl$, K_2CO_3, DMF, 90 °C, 12 h. iv) 100% $NH_2NH_2{\cdot}H_2O$, methanol, reflux, 6 h. v) Appropriate isothiocynate, ethanol, reflux 1 h. vi) Ethyl bromoacetate, anhydrous sod. acetate, reflux 5 h.

antibody that is particular to TUBb. Subsequently, each microplate well was provided with Avidin conjugated to [Horseradish Peroxidase (HRP)] and incubated. After adding TMB substrate solution, only those wells containing TUBb, biotin-conjugated antibody and enzyme-conjugated Avidin will show color change. The reaction was terminated through adding sulfuric acid solution and the change in color was determined spectrophotometrically at a wavelength of [450 nm ± 10 nm]. The TUBb concentration was measured through comparing the O.D. of the samples to the standard curve (Liliom et al., 1995).

2.3.6. Annexin V-FITC apoptosis assay

The MCF-7cells were sowed as mentioned above, incubated with

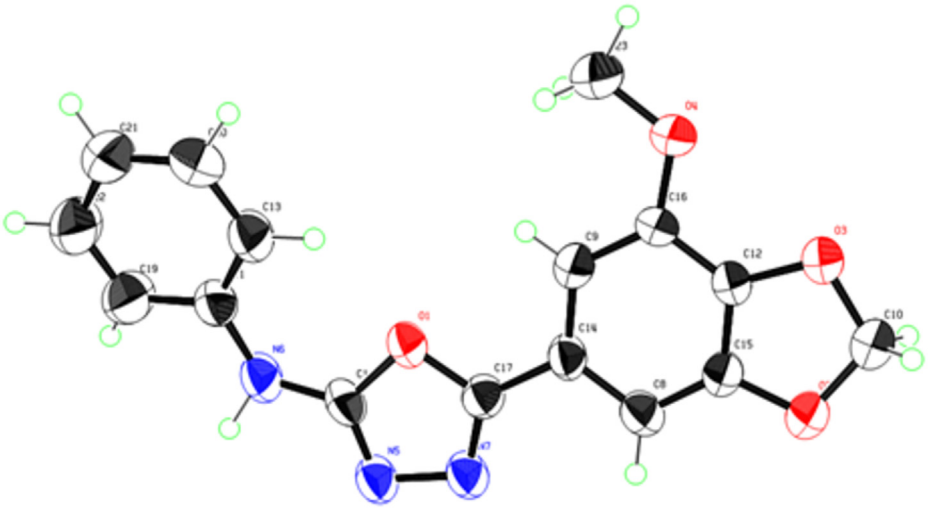

Fig. 2. ORTEP diagram of **10a** with thermal ellipsoids drawn at 50% probability.

compound **11a** at its IC_{50}, collected, washed twice with PBS and then centrifuged. Treatment of cells [10^5 of cells] with Annexin V-FITC and propidium iodide (PI) through apoptosis detection kit [BD Biosciences, San Jose, CA]. The binding of both Annexin V-FITC and PI was investigated using flow cytometry on FACScalibur [BD Biosciences, San Jose, CA]. Logarithmic amplification for FL1 (FITC) and FL2 (PI) channels was used for data gathering. CellQuest software was used for performing quadrant analysis of co-ordinate dot plots. Cells which are unstained were used for adjusting the photomultiplier voltage and abolishing spectral overlap among the FL1 and the FL2 signals (Eldehna et al., 2015).

2.3.7. *In vitro measurement for the concentration of p53, Bax and Bcl-2 proteins*

In vitro measurement for the concentration of p53, Bax and Bcl-2 proteins p53 ELISA kit, Human Bax ELISA kit and Bcl-2 Elisa kit, respectively were used to measure the tumor suppressor gene p53, apoptotic markers Bax and the antiapoptotic marker Bcl-2 levels. Concisely, Cell lysates were set from control and MCF-7 cells [2×10^5/mL] after treatment with compound **11a** at IC_{50} concentration. Then, the same amounts of cell lysates were loaded and probed with specific antibodies. Samples were measured at [450 nm in ROBONEK P2000 ELISA reader], All experiments were performed in triplicates (Nowar et al., 2018).

2.3.8. *Measurement of caspases levels*

The effect of compound **11a** on the level of caspases 3/7, 8 and 9 in MCF-7 cell line was evaluated at its IC_{50} concentration using [Caspase-glo 3/7 Assay kit (Promega), Caspase 8 Human ELISA kit (BMS2024) and Caspase 9 Human ELISA kit (BMS2025)] measured on ROBONIK P2000 (India) spectrophotometer at 450 nm against untreated control cells (negative control) using standard protocols of the manufacturer (Nowar et al., 2018).

2.3.9. *Determination of cytochrome C level*

The level of cytochrome C on MCF-7 cell line after treatment with compound **11a** at its IC_{50} concentration was determined using ab119521 –Cytochrome c Human ELISA Kit according to manufacturer's procedure.

2.4. *Docking studies*

Molecular docking study was performed using discovery studio domain 2016. The 3D crystal structure of tubulin (PDB code: ISA0), was downloaded from PDB followed by protein preparation and addition of hydrogen atoms. The binding site of the selected co-crystallized ligand (colchicine) was created as volumes. Before docking water molecules were omitted from the protein and the tested compounds were minimized energetically using CHARMm Force Field through ligand minimization tool. Docking was accomplished according to protocol settings defaulting.

3. Results and discussion

3.1. *Chemistry*

The synthetic strategy of the target candidates 1,3-benzodioxoles and 1,4-benzodioxines and their intermediates is shown in Scheme 1. Gallic acid (**1**) was esterified using *p*-toluene sulfonic acid as a catalyst to obtain the methyl ester **2** (Mostafa et al., 2006). The latter was subjected to selective etherification using borax and dimethyl sulfate to obtain methyl 5-methoxygallate (**3**) (Pettit and Singh, 1987). Subsequent cyclization of **3** using dichloromethane or 1,2-dichloroethane gave the corresponding 1,3-benzodioxole and 1,4-benzodioxine derivatives **4a** (Zhang et al., 2007) and **4b** (Tsyganov et al., 2013), respectively. Hydrazinolysis of **4a** or **4b** gave the corresponding hydrazides **5a** (Semenov et al., 2010) and **5b**. The synthesis of the new thiosemicarbazides **6a–e** and **7a–e** was achieved through the reaction of hydrazides **5a** or **5b** with the appropriate isothiocyanate in ethanol. IR spectra of thiosemicarbazides **6a–e** and **7a–e** showed three bands at 3746–3167 cm^{-1} for three NH. Also the structures of the latter compounds were proved using ^1H NMR by the presence of singlet signals of NH at 8.00–10.45 ppm.

In agreement with Cesur et al. (1992) reaction of thiosemicarbazides **6a**, **b** or **7a**, **b** (where R = alkyl) with ethyl bromoacetate in presence of anhydrous sodium acetate yielded the target thiazolidinones **8a**, **b** and **9a**, **b**, respectively. Meanwhile, the same reaction with 4-arylthiosemicarbazides **6c–e** or **7c–e** gave 1,3,4-oxadiazoles **10a–c** and **11a–c**, respectively. The structures of the new thiazolidinones **8a**, **b** and **9a**, **b** were confirmed in ^1H NMR by presence of singlet signal of CH_2 between 3.6 and 4 ppm as well as in ^{13}C NMR by appearance of new signal at 30 ppm. The single crystal X-ray study of compound **10a** (CCDC: 1907714) also proved the formation of 1,3,4-oxadiazole ring (Fig. 2) (Table 1). The structures of the new intermediates and target compounds were further substantiated using different spectral data and elemental analyses.

Table 1
Crystal data and structure refinement for **10a**.

CCDC number	1907714
Crystal data	
Chemical formula	$C_{16}H_{13}N_3O_4$
Molecular weight	311.297
Temperature	298 K
Wavelength	0.71073
Crystal system	Triclinic
Space group	*P*ī
Cell dimensions	a = 6.0093 (3) Å b = 10.3447 (5) Å c = 12.8800 (7) Å α = 110.276 (3)° β = 96.473 (3)°, γ = 97.463 (3)°
Volume	733.91 (6) Å^3
Z	2
Radiation type	Mo Kα
Absorption coefficient	0.104 mm^{-1}
Density	1.409 Mg m^{-3}
Crystal size	0.17 × 0.48 × 0.18 mm
Data collection	
T min, *T* max	0.842, 0.983
F000	324
Index range	−8 ≤ h ≤ 8, −14 ≤ k ≤ 13, 0 ≤ l ≤ 18
Absorption correction	Multi scan
No. of measured, independent and observed [$I > 2.0\ \sigma\ (I)$] reflections	4186, 4186, 1109
Refinement	
Refinement method	Full matrix least square on F^2
No. of parameters	208
R [F^2 > 2.0 σ (F^2)], w*R* (F^2), S	0.0575, 0.2016, 0.648
$\Delta\rho_{max}$, $\Delta\rho_{min}$	0.161, −0.169 eÅ^3

3.2. Biological evaluation

3.2.1. Cytotoxic activity

The antiproliferative activity of 1,3-benzodioxoles and 1,4-benzodioxines **8a**, **b**, **9a**, **b**, **10a–c** and **11a–c** is presented in Table 2. This study was performed on four human cancer cell lines A549, MCF-7, PC-3 and HepG2 which are derived from human lung, breast, prostate and liver tumors, respectively using MTT assay (Mosmann, 1983). The 1,4-benzodioxine oxadiazole hybrid **11a** exhibited the highest cytotoxic effect against all the tested cell lines with IC_{50} < 10 µM, while its 1,3-benzodioxole homologue **10a** had good to moderate anticancer activity with IC_{50} ranged between 6.56 and 67.70 µM with higher selectivity on A549 cell line. Generally, compounds bearing the 4-thiazolidinone ring **8a**, **b** and **9a**, **b** were devoid of anticancer activity. Meanwhile, the congeners having 1,3,4-oxadiazole ring **10a–c** and **11a–c** exhibited variable anticancer effect. The substitution on the phenyl ring in 1,3,4-oxadiazole derivatives **10a–c** and **11a–c** with either electron donating or withdrawing group decreased the anticancer potential. Conclusively, the 1,4-benzodioxine oxadiazole hybrids **11a–c** displayed better cytotoxic effect than the 1,3-benzodioxole homologues **10a–c** on most of the tested cell lines.

Table 3
Selectivity index values for compounds **10a** and **11a** relative to BJ1 cell line.

Compound	A549	MCF-7	PC-3	HepG2
10a	16.82	1.63	4.75	3.21
11a	5.64	7.59	5.25	5.98

On the other hand, the derivatives which displayed remarkable anticancer activity **10a** and **11a** were selected to determine their cytotoxicity on human normal cell line BJ1 (skin fibroblasts) (Table 3). Selectivity indices of these compounds on each cancer cell line were calculated relative to BJ1 cell line and presented in Table 3. According to Suffness findings (Suffness, 1990) the compound is considered to be selective if it has selectivity index > 2. From the calculated values compound **10a** has the highest selectivity on A549, however its selectivity on MCF-7 is poor. Meanwhile, compound **11a** has good selectivity on all the tested cancer cell lines relative to normal cell line (Table 3).

3.2.2. Cell cycle analysis

Compound **11a** which is the most active one was selected to investigate its effect on the cell cycle progression of MCF-7 cells at its IC_{50} using flowcytometry. DNA content analysis using propidium iodide showed that compound **11a** produced a raise in the percentage of cells at pre-G1 by 16.8-folds in comparison with the untreated cells which is a significant marker of apoptosis. In addition, compound **11a** interfered with the cell cycle at G2/M phase causing cells accumulation 4.4 folds more than the control (Fig. 3).

3.2.3. Effect on tubulin polymerization

Antimitotic drugs are widely used in management of metastatic breast cancer (Davidson, 1995; Kennedy et al., 1995). It has been reported that compounds which cause arrest in cell cycle at G2/M phase have an influence on tubulin assembly (Kanthou et al., 2004). Thus, the mode of action of the most active derivative **11a** was investigated by determination of its tubulin polymerization inhibitory effect. Colchicine was used as a reference compound and the IC_{50} values were calculated as shown in Table 4. Compound **11a** exhibited tubulin polymerization inhibition activity with IC_{50} 6.37 µM.

Table 2
Anticancer effect of the new 1,3-benzodioxole and 1,4-benzodioxine derivatives on different human cell lines.

Compound	IC_{50} (µM)[a]				
	A549	MCF-7	PC-3	HepG2	BJ1
8a	> 100	> 100	> 100	> 100	ND
8b	> 100	> 100	> 100	> 100	ND
9a	> 100	> 100	> 100	> 100	ND
9b	> 100	> 100	> 100	> 100	ND
10a	6.56 ± 0.19	67.70 ± 1.12	23.23 ± 1.66	34.40 ± 0.16	110.40 ± 4.66
10b	66.05 ± 1.91	> 100	> 100	> 100	ND
10c	27.62 ± 0.18	> 100	57.86 ± 0.81	54. 09 ± 0.20	ND
11a	7.94 ± 0.15	5.90 ± 0.51	8.53 ± 0.64	7.49 ± 0.32	44.80 ± 2.64
11b	56.21 ± 2.88	> 100	> 100	> 100	ND
11c	14.11 ± 1.23	24.87 ± 0.07	42.55 ± 0.19	27.92 ± 1.11	ND
Doxorubicin	3.01 ± 0.18	4.21 ± 0.21	6.77 ± 0.24	3.52 ± 0.11	ND

ND: not determined.
[a] IC_{50} values are the mean ± S.D. of three separate experiments.

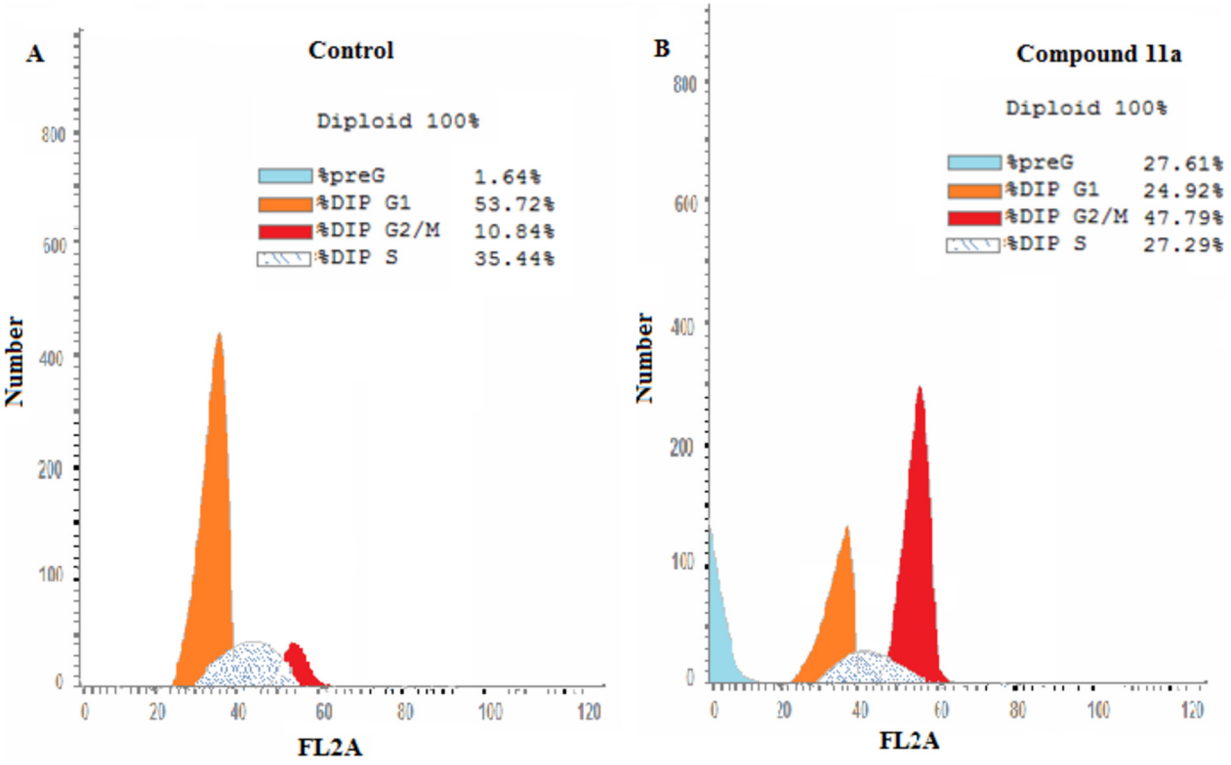

Fig. 3. Flow cytometry analysis for MCF-7 cells. A) Control cells, B) cells after treatment with compound **11a** at its IC_{50} concentration.

Table 4
Inhibition of tubulin polymerization (IC_{50}) of compound **11a**.

Comp.	IC_{50} ± SD (μM)[a]
11a	6.37 ± 0.29
Colchicine	4.13 ± 0.22

[a] IC_{50} values are the mean ± S.D. of three separate experiments.

3.2.4. Annexin V-FITC apoptosis assay

During apoptosis phosphatidylserine (PS) in the inner plasma membrane loses its asymmetric distribution and translocates to the outer membrane. Annexin V/PI assay can be used to identify apoptotic cells because annexin V preferentially binds to PS (Andree et al., 1990). The plasma membrane of the cells at early apoptosis excludes viability dyes such as propidium iodide (PI). Thus, cells in early apoptosis will be stained by annexin V but not with PI (Annexin V positive, PI-negative). However, the cell membrane loses integrity in late-stage apoptosis and the cells will be stained with both types of dyes (Annexin V positive, PI-positive). Treatment of MCF-7 cell line with 5.90 μM of compound **11a** resulted in an increase in cells at early-stage apoptosis by 8.7 folds comparing to control. Also the percentage of cells in late apoptosis increased from 0.33% in control cells to 19.02% in treated ones (Fig. 4).

3.2.5. Measurement of apoptosis regulatory molecules

3.2.5.1. Effect on Bcl-2 family members. The Bcl-2 proteins are divided into proteins that promote apoptosis like Bax and others inhibit apoptosis like Bcl-2 (Perlman et al., 1999; Frenzel et al., 2009). Generally Bcl-2 family proteins play a role in regulating apoptosis by controlling the mitochondrial membrane permeability (Brunelle and Letai, 2009). Apoptosis is attenuated by antiapoptotic members of this group of proteins such as Bcl-2 through decreasing mitochondrial apoptogenic factors release such as cytochrome *c* into cytoplasm. While, Bcl-2 family pro-apoptotic members as Bax cause caspases release (Youle and Strasser, 2008). The Bcl-2 and Bax levels were determined in MCF-7 cells after treatment with compound **11a** to study its ability to enhance apoptosis. It was found that levels of Bcl-2 protein were down-regulated to its half value compared to control after treatment with compound **11a**. On the other hand, exposure of the tested cells to compound **11a** yielded about 10 folds increase of Bax protein expression. From these results it was found that Bax/Bcl-2 ratio was elevated comparing with control indicating the ability of compound **11a** to induce apoptosis (Table 5).

3.2.5.2. Effect on level of p53. It has been reported that expression of Bcl-2 and Bax genes is controlled through tumor suppressor gene p53 (Miyashita et al., 1994). After treatment with compound **11a**, the level of tumor suppressor gene p53 expression was determined in MCF-7 cells. The tested compound could promote the expression of tumor suppressor gene p53 by 11.8 folds compared to control (Table 5).

3.2.5.3. Measurement of caspases levels. Caspases are cysteine containing proteases which hydrolyze substrate at aspartic acid residues. This group of enzymes provides a vital role in controlling cell death. There are two pathways of apoptosis either receptor-mediated (extrinsic) or mitochondrial mediated (intrinsic). Caspases is classified as either initiator caspases (caspase-8 and -9) or executioner ones (caspase-3, -6, and -7). Extrinsic and intrinsic apoptosis lead to activation of initiator caspases 8 and 9, respectively (Chen and Wang, 2002). Consequently, these two initiator caspases 8 and 9 trigger the activation of executioner caspases-3/6/7 (Parrish et al., 2013). Elevated Bax/Bcl2 ratio for compound **11a** encouraged to measure its effect on the levels of both initiator caspases 8 and 9 and executioner caspases-3/7 in MCF-7 cells. Treatment of the cells with IC_{50} concentration of compound **11a** caused significant increase in levels of caspases 8, 9, and 3/7 by 4.5, 20.2, 3.9 folds, respectively comparing with negative control. These findings suggest that compound **11a** elicit both extrinsic and intrinsic apoptotic pathways in MCF-7 cells.

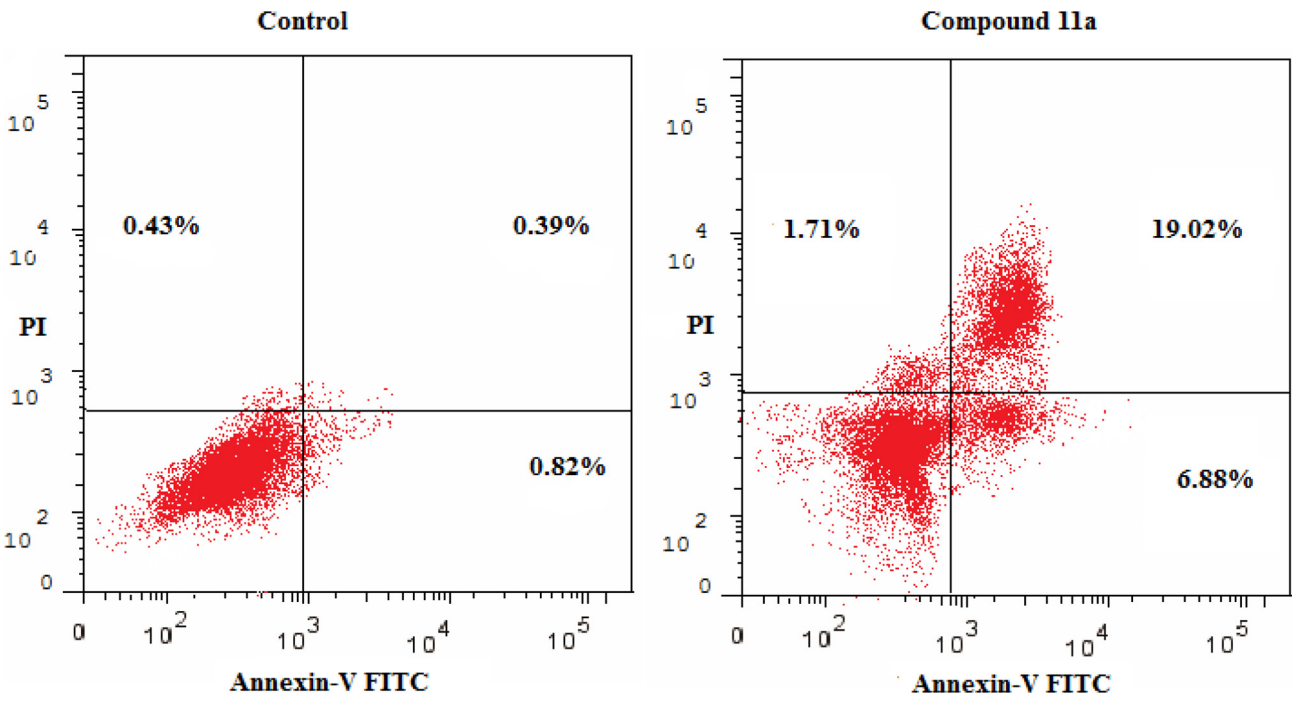

Fig. 4. Effect of compound **11a** on percentage of apoptotic cells in MCF-7 cells using Annexin V/PI double staining.

3.2.5.4. Determination of cytochrome C level. Upon increase of the Bax/Bcl-2 ratio the cytochrome C is released into the cytoplasm and it triggers the executioner caspases (Shimizu et al., 1999). Measurement of cytochrome C level in MCF-7 cells after incubation with derivative **11a** revealed significant increase in its amount by 7.6 folds compared to untreated cells. This result is in accordance with the above-mentioned increase in executioner caspases level.

3.3. Molecular modeling study

Molecular docking study was performed to understand the binding and interactions of derivative **11a** inside the colchicine binding site of tubulin (PDB ID: 1SA0) using Discovery studio 2016 (Ahmed et al., 2017). DAMA-colchicine binding site contains two hydrophobic cavities bind to the phenyl and tropone rings of the co-crystallized ligand. Analysis of docking results of compound **11a** showed that it had a comparable CDOCKER energy with that of the reference ligand. Besides, it interacted with various amino acids reported previously in docking studies of CSIs (Ahmed et al., 2017; El-Sherief et al., 2018). The most active compound **11a** showed good shape complimentarily in the active binding site and having five hydrogen bonds (two hydrogen bonds with Asn 258, two hydrogen bond with Asn 350 and one hydrogen with val 315 residues). Moreover, it forms van der Waals interaction with Leu 242, Val 238, Val 318, Val 351, Met 259, Ile 378 and pi-alkyl interaction with Leu 248, Lys 254, Lue 255 and Ala 250 as well as pi-sulfur interaction with Cys241 (Fig. 5).

4. Conclusion

In this study novel derivatives of 1,3-benzodioxole and its higher homologue 1,4-benzodioxine hybridized with 1,3,4-oxadiazole or thiazolidin-4-one rings were synthesized and evaluated as anticancer agents against HepG2, PC-3, MCF-7 and A549 human cancer cell lines. The 1,4-benzodioxine derivative **11a** is the most active compound with a broad spectrum activity towards the four tested cancer cell lines (IC_{50} < 10 μM) and it displayed lower toxic effect on normal human cell line BJ1. Flow cytometeric analysis showed that compound **11a** induced accumulation of MCF-7 cells at G2/M phase as well as considerable increase in the cells percentage at pre-G1. Compound **11a** is proved to possesses a tubulin polymerization inhibitory effect with IC_{50} = 6.37 μM. This compound could induce both early and late stage apoptosis in MCF-7 cells. Also, the ability of this compound to stimulate apoptosis in the latter cell line was further confirmed by increment of Bax/Bcl-2 ratio, increase the expression of tumor suppressor gene p53, boosting the levels of initiator and executioner caspases as well as raise in the amount of cytochrome C. Furthermore, molecular docking of compound **11a** was performed on the colchicine binding site of tubulin to investigate its binding mode to the target receptor. These findings encouraged the future profound investigation of 1,3-benzodioxole and 1,4-benzodioxine derivatives in order to produce anticancer agents having either of these moieties.

Acknowledgments

The authors would like express their thanks to the National Research Centre, Dokki, Giza, Egypt for supporting this work under the

Table 5
Influence of compound **11a** on the expression levels of apoptosis regulatory molecules in MCF-7 cell line.[a]

Comp.	Bax ng/mL	Bcl-2 ng/mL	p53 ng/mL	Caspase 8 ng/mL	Caspase 9 ng/mL	Caspase 3/7 ng/mL	Cytochrome C ng/mL
11a	0.21	2.91	0.53	0.73	13.33	0.47	0.76
Control	0.02	5.83	0.04	0.16	0.65	0.12	0.10

[a] All experiments were performed at IC_{50} concentration of **11a** on MCF-7 cell line.

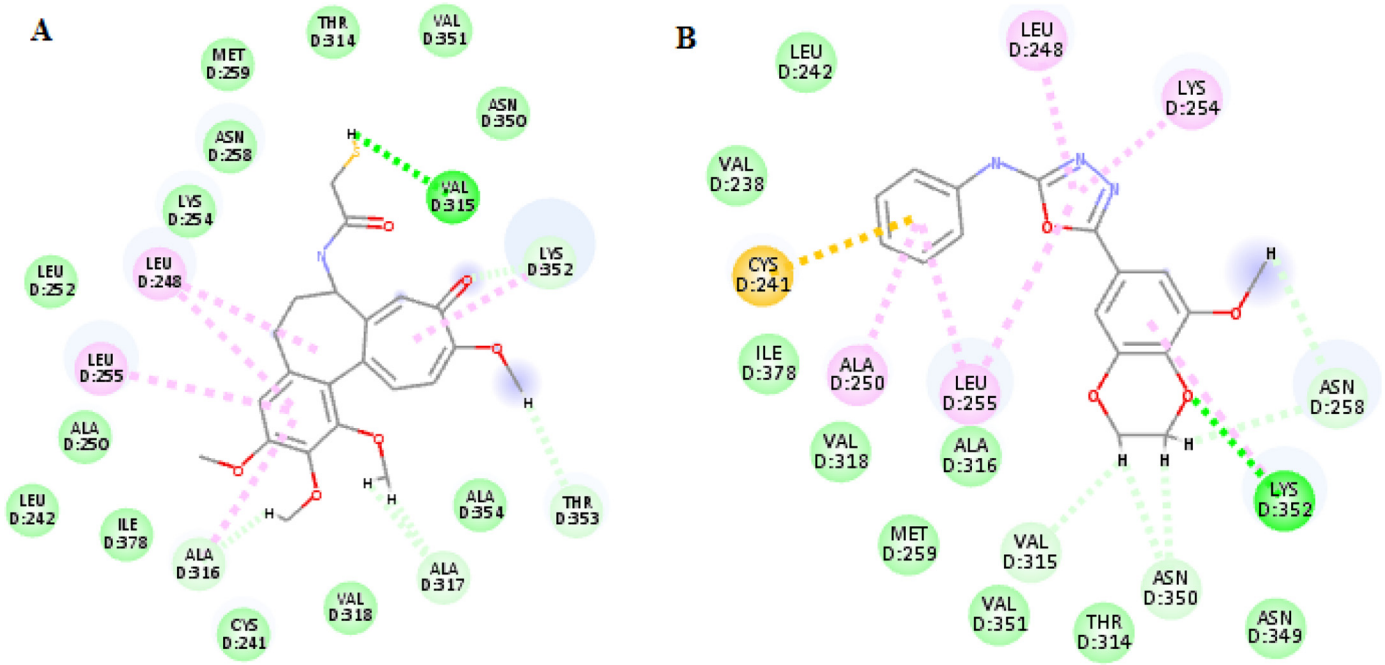

Fig. 5. 2D Interaction diagram (A) for co-crystallized ligand colchicine (B) for compound **11a**.

project no. 11010311.

Declaration of competing interest

Authors have no conflict of interest to declare.

Appendix A. Supplementary data

Supplementary data to this article can be found online at https://doi.org/10.1016/j.ejps.2019.105045.

References

Aboul-Enein, M.N., El-Azzouny, A.A.S., Saleh, O.A., Amin, K.M., Maklad, Y.A., Hassan, R.M., 2015. Synthesis and anticonvulsant activity of substituted-1,3-diazaspiro[4.5] decan-4-ones. Arch. Pharm. 348, 575–588.
Ahmed, R.I., Osman, E.E., Awadallah, F.M., El-Moghazy, S.M., 2017. Design, synthesis and molecular docking of novel diarylcyclohexenone and diarylindazole derivatives as tubulin polymerization inhibitors. J. Enzyme. Inhib. Med. Chem. 32, 176–188.
Altomare, A., Cascarano, G., Giacovazzo, C., Guagliardi, A., Burla, M., Polidori, G.t., Camalli, M., 1994. SIRPOW. 92–a program for automatic solution of crystal structures by direct methods optimized for powder data. J. Appl. Crystallogr. 27, 435–436.
Andree, H., Reutelingsperger, C., Hauptmann, R., Hemker, H.C., Hermens, W.T., Willems, G., 1990. Binding of vascular anticoagulant alpha (VAC alpha) to planar phospholipid bilayers. J. Bio. Chem. 265, 4923–4928.
Batra, J.K., Jurd, L., Hamel, E., 1985. Structure-function studies with derivatives of 6-benzyl-1,3-benzodioxole, a new class of synthetic compounds which inhibit tubulin polymerization and mitosis. Mol. Pharmacol. 27, 94–102.
Botta, M., Forli, S., Magnani, M., Manetti, F., 2008. Molecular Modeling Approaches to Study the Binding Mode on Tubulin of Microtubule Destabilizing and Stabilizing Agents Tubulin-binding Agents. Springer, pp. 279–328.
Brunelle, J.K., Letai, A., 2009. Control of mitochondrial apoptosis by the Bcl-2 family. J. Cell. Science 122, 437–441.
Cesur, N., Cesur, Z., Gursoy, A., 1992. New acylthiosemicarbazides, thiazolidinones, and 1,3,4-oxadiazoles as possible anticonvulsants. Arch. Pharm (Weinheim). 325, 623–624.
Chen, M., Wang, J., 2002. Initiator caspases in apoptosis signaling pathways. Apoptosis 7, 313–319.
Davidson, N.G., 1995. Single-agent Paclitaxel at First Relapse Following Adjuvant Chemotherapy for Breast Cancer. (Paper presented at the Seminars in oncology).
Desbène, S., Giorgi-Renault, S., 2002. Drugs that inhibit tubulin polymerization: the particular case of podophyllotoxin and analogues. Curr. Med. Chem. Anti-Cancer Agents 2, 71–90.
Downing, K.H., Nogales, E., 1998. Tubulin structure: insights into microtubule properties and functions. Cur. Opin. Struc. Biol. 8, 785–791.
Eldehna, W.M., Ibrahim, H.S., Abdel-Aziz, H.A., Farrag, N.N., Youssef, M.M., 2015. Design, synthesis and in vitro antitumor activity of novel N-substituted-4-phenyl/benzylphthalazin-1-ones. Eur. J. Med. Chem. 89, 549–560.
El-Sherief, H.A.M., Youssif, B.G.M., Bukhari, S.N.A., Abdel-Aziz, M., Abdel-Rahman, H.M., 2018. Novel 1,2,4-triazole derivatives as potential anticancer agents: design, synthesis, molecular docking and mechanistic studies. Bioorg. Chem. 76, 314–325.
Fan, A., Wei, J., Yang, M., Zhang, Q., Zhang, Y., Liu, Q., Li, J., 2018. Pharmacodynamic and pharmacokinetic characteristics of YMR-65, a tubulin inhibitor, in tumor-bearing mice. Eur. J. Pharm. Sci. 121, 74–84.
Frenzel, A., Grespi, F., Chmelewskij, W., Villunger, A., 2009. Bcl2 family proteins in carcinogenesis and the treatment of cancer. Apoptosis 14, 584–596.
Hao, Y.-p., Liu, Z.-y., Xie, C., Zhou, L., Sun, X., 2016. Novel fluorinated docetaxel analog for anti-hepatoma: molecular docking and biological evaluation. Eur. J. Pharm.Sci. 88, 274–281.
Jayashankar, B., Lokanath Rai, K.M., Baskaran, N., Sathish, H.S., 2009. Synthesis and pharmacological evaluation of 1,3,4-oxadiazole bearing bis(heterocycle) derivatives as anti-inflammatory and analgesic agents. Eur. J. Med. Chem. 44, 3898–3902.
Kamal, A., Srikanth, Y., Shaik, T.B., Khan, M.N.A., Ashraf, M., Reddy, M.K., Kalivendi, S.V., 2011. 2-Anilinonicotinyl linked 1,3,4-oxadiazole derivatives: synthesis, anti-tumour activity and inhibition of tubulin polymerization. Med.Chem.Comm. 2, 819–823.
Kamal, A., Srikanth, P.S., Vishnuvardhan, M.V., Kumar, G.B., Suresh Babu, K., Hussaini, S.M., Alarifi, A., 2016. Combretastatin linked 1,3,4-oxadiazole conjugates as a potent tubulin polymerization inhibitors. Bioorg. Chem. 65, 126–136.
Kanthou, C., Greco, O., Stratford, A., Cook, I., Knight, R., Benzakour, O., Tozer, G., 2004. The tubulin-binding agent combretastatin A-4-phosphate arrests endothelial cells in mitosis and induces mitotic cell death. Am. J. Pathol. 165, 1401–1411.
Kennedy, M.J., Donehower, R.C., Rowinsky, E.K., 1995. Treatment of metastatic breast cancer with combination paclitaxel/cyclophosphamide. In: Paper Presented at the Seminars in Oncology.
Kiselyov, A.S., Semenova, M.N., Chernyshova, N.B., Leitao, A., Samet, A.V., Kislyi, K.A., Semenov, V.V., 2010. Novel derivatives of 1,3,4-oxadiazoles are potent mitostatic agents featuring strong microtubule depolymerizing activity in the sea urchin embryo and cell culture assays. Eur. J. Med. Chem. 45, 1683–1697.
La Regina, G., Coluccia, A., Naccarato, V., Silvestri, R., 2019. Towards modern anticancer agents that interact with tubulin. Eur. J. Pharm. Sci. 131, 58–68.
Li, W., Sun, H., Xu, F., Shuai, W., Liu, J., Xu, S., Xu, J., 2019. Synthesis, molecular properties prediction and biological evaluation of indole-vinyl sulfone derivatives as novel tubulin polymerization inhibitors targeting the colchicine binding site. Bioorg. Chem. 85, 49–59.
Liliom, K., Lehotzky, A., Molnar, A., Ovadi, J., 1995. Characterization of tubulin-alkaloid interactions by enzyme-linked immunosorbent assay. Anal. Biochem. 228, 18–26.
Lu, Y., Chen, J., Xiao, M., Li, W., Miller, D.D., 2012. An overview of tubulin inhibitors that interact with the colchicine binding site. Pharm. Res. 29, 2943–2971.
Mackay, S., Gilmore, C., Edwards, C., Stewart, N., Shankland, K., 1999. maXus Computer Program for the Solution and Refinement of Crystal Structures. Bruker Nonius, The Netherlands, MacScience.
Miyashita, T., Krajewski, S., Krajewska, M., Wang, H.G., Lin, H., Liebermann, D.A., Reed, J.C., 1994. Tumor suppressor p53 is a regulator of bcl-2 and bax gene expression in vitro and in vivo. Oncogene 9, 1799–1805.
Mosmann, T., 1983. Rapid colorimetric assay for cellular growth and survival: application to proliferation and cytotoxicity assays. J. Immunol. Methods 65, 55–63.
Mostafa, M., Nahar, N., Mosihuzzaman, M., Sokeng, S.D., Fatima, N., Atta Ur, R.,

Choudhary, M.I., 2006. Phosphodiesterase-I inhibitor quinovic acid glycosides from Bridelia ndellensis. Nat. Prod. Res. 20, 686–692.
Mu, Y., Liu, Y., Li, L., Tian, C., Zhou, H., Zhang, Q., Yan, B., 2015. The novel tubulin polymerization inhibitor MHPT exhibits selective anti-tumor activity against rhabdomyosarcoma in vitro and in vivo. PLoS One 10, e0121806.
Nowar, R.M., Osman, A., E, E., Abou-Seri, S.M., El Moghazy, S.M., Abou El Ella, D.A., 2018. Design, synthesis and biological evaluation of some novel quinazolinone derivatives as potent apoptotic inducers. Future. Med. Chemistry 10, 1191–1205.
Palatinus, L., Chapuis, G., 2007. SUPERFLIP–a computer program for the solution of crystal structures by charge flipping in arbitrary dimensions. J. Appl. Crystallogr. 40, 786–790.
Parrish, A.B., Freel, C.D., Kornbluth, S., 2013. Cellular mechanisms controlling caspase activation and function. Cold Spring Harb. Perspect. Biol. 5 (6).
Patel, N.B., Purohit, A.C., Rajani, D.P., Moo-Puc, R., Rivera, G., 2013. New 2-benzylsulfanyl-nicotinic acid based 1,3,4-oxadiazoles: their synthesis and biological evaluation. Eur. J. Med. Chem. 62, 677–687.
Perlman, H., Zhang, X., Chen, M.W., Walsh, K., Buttyan, R., 1999. An elevated bax/bcl-2 ratio corresponds with the onset of prostate epithelial cell apoptosis. Cell Death Differ. 6, 48–54.
Pettit, G.R., Singh, S.B., 1987. Isolation, structure, and synthesis of combretastatin A-2, A-3, and B-2. Can. J. Chem. 65, 2390–2396.
Pettit, G., Singh, S., Hamel, E., Lin, C.M., Alberts, D.S., Garcia-Kendal, D., 1989. Isolation and structure of the strong cell growth and tubulin inhibitor combretastatin A-4. Experientia 45, 209–211.
Pettit, G.R., Temple, J.C., Narayanan, V., Varma, R., Simpson, M., Boyd, M., Bansal, N., 1995. Antineoplastic agents 322. Synthesis of combretastatin A-4 prodrugs. Anticancer Drug Des. 10, 299–309.
Rashid, M., Husain, A., Mishra, R., 2012. Synthesis of benzimidazoles bearing oxadiazole nucleus as anticancer agents. Eur. J. Med. Chem. 54, 855–866.
Rigo, B., Couturier, D., 1985. Studies on pyrrolidinones. Synthesis of 5-(5-oxo-2-pyrrolidinyl)-1,3,5-oxadiazole-2-thione derivatives. J. Heterocyclic Chem. 22, 287–288.
Semenov, V.V., Kiselyov, A.S., Titov, I.Y., Sagamanova, I.K., Ikizalp, N.N., Chernysheva, N.B., Semenova, M.N., 2010. Synthesis of antimitotic polyalkoxyphenyl derivatives of combretastatin using plant allylpolyalkoxybenzenes. J. Nat. Prod. 73, 1796–1802.
Sheldrick, G.M., 2008. A short history of SHELX. Acta. Crystallogr A. 64, 112–122.
Shimizu, S., Narita, M., Tsujimoto, Y., 1999. Bcl-2 family proteins regulate the release of apoptogenic cytochrome c by the mitochondrial channel VDAC. Nature 399, 483–487.
Stengel, C., Newman, S., Leese, M., Potter, B., Reed, M., Purohit, A., 2010. Class III β-tubulin expression and in vitro resistance to microtubule targeting agents. Brit. J. Cancer 102, 316–324.
Suffness, M., 1990. Assays related to cancer drug discovery. Methods in Plant Biochemistry: Assays for Bioactivity 6, 71–133.
Torre, L.A., Bray, F., Siegel, R.L., Ferlay, J., Lortet-Tieulent, J., Jemal, A., 2015. Global cancer statistics, 2012. CA: A Cancer. J. Clin. 65, 87–108.
Trivedi, P., Adhikari, N., Amin, S.A., Jha, T., Ghosh, B., 2018. Design, synthesis and biological screening of 2-aminobenzamides as selective HDAC3 inhibitors with promising anticancer effects. Eur. J.Pharm. Sci. 124, 165–181.
Tsyganov, D.V., Konyushkin, L.D., Karmanova, I.B., Firgang, S.I., Strelenko, Y.A., Semenova, M.N., Semenov, V.V., 2013. cis-Restricted 3-aminopyrazole analogues of combretastatins: synthesis from plant polyalkoxybenzenes and biological evaluation in the cytotoxicity and phenotypic sea urchin embryo assays. J. Nat. Prod. 76, 1485–1491.
Yi, X., Zhong, B., Smith, K.M., Geldenhuys, W.J., Feng, Y., Pink, J.J., Su, B., 2012. Identification of a class of novel tubulin inhibitors. J. Med. Chem. 55, 3425–3435.
Youle, R.J., Strasser, A., 2008. The BCL-2 protein family: opposing activities that mediate cell death. Nat. Rev. Mol. Cell Biol. 9, 47–59.
Zhang, W.G., Zhao, R., Ren, J., Ren, L.X., Lin, J.G., Liu, D.L., Yao, X.S., 2007. Synthesis and anti-proliferative in-vitro activity of two natural dihydrostilbenes and their analogues. Arch. Pharm (Weinheim). 340, 244–250.
Zhang, Q., Liu, X., Li, X., Li, C., Zhou, H., Yan, B., 2013. Antitumor activity of (2E,5Z)-5-(2-hydroxybenzylidene)-2-((4-phenoxyphenyl)imino) thiazolidin-4-one, a novel microtubule-depolymerizing agent, in U87MG human glioblastoma cells and corresponding mouse xenograft model. J. Pharmacol. Sci. 122, 223–231.